

Simulating quantum circuit expectation values by Clifford perturbation theory

Tomislav Begušić, Kasra Hejazi, and Garnet Kin-Lic Chan

Division of Chemistry and Chemical Engineering, California Institute of Technology, Pasadena, California 91125, USA

July 12, 2023

The classical simulation of quantum circuits is of central importance for benchmarking near-term quantum devices. The fact that gates belonging to the Clifford group can be simulated efficiently on classical computers has motivated a range of methods that scale exponentially only in the number of non-Clifford gates. Here, we consider the expectation value problem for circuits composed of Clifford gates and non-Clifford Pauli rotations, and introduce a heuristic perturbative approach based on the truncation of the exponentially growing sum of Pauli terms in the Heisenberg picture. Numerical results are shown on a Quantum Approximate Optimization Algorithm (QAOA) benchmark for the E3LIN2 problem and we also demonstrate how this method can be used to quantify coherent and incoherent errors of local observables in Clifford circuits. Our results indicate that this systematically improvable perturbative method offers a viable alternative to exact methods for approximating expectation values of large near-Clifford circuits.

1 Introduction

Validating near-term quantum devices with classical simulations is paramount for their future development [1]. In general, the classical simulation of quantum circuits is hard and thus limited to a small number of qubits or gates. One exception is Clifford circuits, which can be simulated efficiently using the stabilizer formalism [2, 3, 4]. From this starting point, circuit simulation methods have been developed which scale exponentially only with the number of non-Clifford gates [5, 6, 7, 8, 9, 10]. Currently, the low-rank stabilizer method proposed by Bravyi et al. [8] is one of the best-scaling methods for sampling the output distribution of a quantum circuit with a small number of non-Clifford gates.

In this work, we are concerned not with sampling the full output distribution of a quantum circuit, but only with evaluating the expectation value (mean value) of Pauli operators. Quantum mean values [11] are not only a central aspect of the quantum output, but also form the cost function in variational quantum algorithms [12], such as the variational quantum eigensolver (VQE) [13] or QAOA [14, 15]. Here, we introduce a technique to obtain expectation values of quantum circuits based on a Clifford-based perturbation

Tomislav Begušić: These authors contributed equally to this work.

Kasra Hejazi: These authors contributed equally to this work.

Garnet Kin-Lic Chan: gkc1000@gmail.com

method. The method is most efficient when the gates are close to Clifford. Specifically, in the proposed heuristic inspired by time-dependent perturbation theory, the general Heisenberg evolution of a Pauli observable is computed as a polynomial in non-Clifford parameters, and the polynomial is truncated to control the cost. We use numerical examples to show that accurate results can be obtained even with low orders of perturbation, and we demonstrate on a QAOA benchmark that the method is faster than computing expectation values by sampling methods by orders of magnitude. Finally, we show how the method can be used to model coherent and incoherent noise in Clifford circuits, which is relevant to benchmarking stabilizer error-correcting codes with many qubits.

2 Method

We consider the expectation value

$$\langle O \rangle = \langle 0^{\otimes n} | C_N^\dagger U_N^\dagger \cdots C_1^\dagger U_1^\dagger O U_1 C_1 \cdots U_N C_N | 0^{\otimes n} \rangle \quad (1)$$

of a Pauli operator O evolved under a set of general unitary operators (quantum gates) U_i and Clifford gates C_i in the Heisenberg picture. For convenience, we label the gates in the order in which they are applied to the operator. Note that since Clifford gates both include the identity and are subsets of general unitary gates, the above expression can represent any quantum circuit with N gates.

Without loss of generality, through circuit compilation we can consider circuits (1) containing only Pauli rotations $U_i \equiv U_i(\theta_i) = \exp(-i\theta_i P_i/2)$, where P_i are Pauli operators, and, further, that the angles satisfy $|\theta_i| \leq \pi/4$. The latter is because for any $|\theta_i| > \pi/4$, we can use the angle transformation $U_i(\theta_i) = U_i(\tilde{\theta}_i + k\pi/2)C_{U_i}$, where $C_{U_i} = \exp(-ik\pi P_i/4)$ ($k \in \mathbb{Z}$) is again a Clifford gate. Similarly, because Clifford gates map the Pauli group onto itself [2], every gate C_i can be applied to the observable O and all $P_{j < i}$ without increasing the number of terms, leaving only Pauli rotations with modified P_i . Applying these two transformations is efficient and yields the Clifford interaction picture, whereby Eq. (1) becomes

$$\langle O \rangle = \langle 0^{\otimes n} | U_N(\theta_N)^\dagger \cdots U_1(\theta_1)^\dagger O U_1(\theta_1) \cdots U_N(\theta_N) | 0^{\otimes n} \rangle \quad (2)$$

with all $|\theta_i| \leq \pi/4$, and the U_i have been transformed by the Cliffords.

To reduce the cost of evaluating Eq. (2), we first note that many circuits possess a certain structure that reduces the number of gates that affect the final expectation value. Specifically, the application of a Pauli rotation to a Pauli operator yields:

$$e^{i\theta P/2} O e^{-i\theta P/2} = \begin{cases} O, & [P, O] = 0, \\ \cos(\theta)O + i \sin(\theta)PO & \{P, O\} = 0. \end{cases} \quad (3)$$

Therefore, only gates that anticommute with the observable increase the number of Pauli terms needed to represent the Heisenberg-evolved observable and thus contribute to the computational cost. The full circuit is applied by iterating Eq. (3), that is, at step $i + 1$, the evolved observable is $O_{i+1} = U_{i+1}(\theta_{i+1})^\dagger O_i U_{i+1}(\theta_{i+1}) = \sum_j U_{i+1}(\theta_{i+1})^\dagger \sigma_{i,j} U_{i+1}(\theta_{i+1})$, where $O_i = \sum_j \sigma_{i,j}$ and $\sigma_{i,j}$ are Pauli operators. The worst-case scaling of this method is 2^N , which is attained only if all P_i anticommute with O and commute with each other. For random circuits, we can expect that P_{i+1} will commute on average with half of the Pauli terms in the evolved observable and generate $M_{i+1} = 3/2 M_i$ Pauli terms, leading to an average scaling of $(3/2)^n$.

In this work, we do not aim to propose an exact or rigorously δ -approximate method with an asymptotic exponential scaling better than that already available in the literature. Rather, we are interested in computing expectation values approximately, but in a systematically improvable way, via a perturbation expansion. For this purpose, we note that the ratio between coefficients of the O and PO branches in Eq. (3) is $\tan(\theta)$. Since $|\theta| \leq \pi/4$, we know that $|\tan(\theta)| \leq 1$, i.e., the two branches will be weighted equally in the worst case, but otherwise, the term involving the unmodified Pauli operator O will be larger. This motivates an ordering of terms by the number of multiplications by $\sin(\theta_i)$, which we call a perturbation order k . We can rewrite the mean value (1) as

$$\langle O \rangle = \sum_{k=0}^{\tilde{N}} E^{(k)}, \quad (4)$$

$$E^{(k)} = i^k \sum_{1 \leq j_1 < j_2 < \dots < j_k \leq \tilde{N}} c_j \sin(\theta_{j_1}) \dots \sin(\theta_{j_k}) \langle 0^{\otimes n} | P_{j_k} \dots P_{j_1} O | 0^{\otimes n} \rangle, \quad (5)$$

where $\tilde{N} \leq N$ is the highest order of perturbation and c_j are products of cosine functions,

$$c_j = \prod_{l \notin \{j_1, \dots, j_k\}}^N \cos^{\xi_l}(\theta_l). \quad (6)$$

In Eq. (6), $\xi_l = 0$ if the Pauli operator P_l , associated with the Pauli rotation gate $U_l(\theta_l)$, commutes with $P_{j_m} \dots P_{j_1} O$ for $j_m < l < j_{m+1}$ and $\xi_l = 1$ otherwise. The goal then is to explore the truncated series

$$\langle O \rangle^{(K)} = \sum_{k=0}^K E^{(k)}, \quad K \leq \tilde{N} \quad (7)$$

as an approximation for $\langle O \rangle$. This series expansion resembles the series expansion of time-dependent perturbation theory, thus we refer to this method as Clifford perturbation theory. The angles $|\tan(\theta)|$ serve as a measure of the non-Clifford nature of the gates and are analogous to perturbation parameters, and the truncated series is thus most accurate for near-Clifford circuits where $|\tan(\theta)| \sim 0$. Note that because the circuit is finite and discrete, unlike in perturbation theories associated with continuous Hamiltonian evolution, the series always truncates at $K = \tilde{N}$ and cannot diverge.

For simplicity, let us consider an example in which all Pauli operators P_i anticommute with O and commute with each other. In this case, $\tilde{N} = N$ and

$$E^{(k)} = i^k \left(\prod_{i=1}^N \cos(\theta_i) \right) \sum_{1 \leq j_1 < j_2 < \dots < j_k \leq N} \tan(\theta_{j_1}) \dots \tan(\theta_{j_k}) \langle 0^{\otimes n} | P_{j_k} \dots P_{j_1} O | 0^{\otimes n} \rangle. \quad (8)$$

On one hand, we can rely on the fact that each term at order k will have an additional factor of $\tan(\theta_{j_k})$ compared to a term at order $k-1$. On the other hand, there are $M_k = \binom{N}{k}$ terms at order k . In practice, however, many terms in Eq. (8) might be zero regardless of the value of θ . For example, for a random Pauli operator P with a weight w the probability of $\langle 0^{\otimes n} | P | 0^{\otimes n} \rangle \neq 0$ is 3^{-w} . Since this possibility is not known before the Pauli operator $P_{j_k} \dots P_{j_1} O$ in (8) is computed, we choose to study this perturbative expansion numerically. In Appendix A, we present a more detailed analysis of the perturbative treatment as applied to random quantum circuits.

We note that a work closely related to ours recently appeared, where the authors consider the truncated Fourier series as an approximation to the quantum mean value

problem [16]. However, their expansion orders terms in Fourier levels that are defined differently from the perturbation series considered in this work. In addition, another perturbative method [17] was proposed for approximately optimizing VQE parameters, in this case, the angles of Pauli rotation gates, in a circuit composed of alternating Pauli and Clifford gates. There, the authors expanded the mean value to second order in the parameters, thereby effectively reducing the problem to a classically efficient Clifford-circuit simulation of the expectation value, its gradient, and Hessian with respect to the parameters.

3 Numerical examples

The Clifford perturbation method was implemented using Qiskit [18] and studied on two different problems. First, we applied the method to evaluate the QAOA cost function of the combinatorial Max E3LIN2 problem [19, 8]. Second, we simulated mean values of a Clifford circuit that was subject to coherent noise, a common source of errors in modern-day implementations of quantum circuits [20].

3.1 QAOA applied to the Max E3LIN2 problem

The Max E3LIN2 problem is a combinatorial optimization task of finding bitstrings z_1, z_2, \dots, z_n that maximize the cost function

$$C_z = \frac{1}{2} \sum_{1 \leq u < v < w \leq n} d_{uvw} z_u z_v z_w, \quad (9)$$

determined by coefficients $d_{uvw} \in \{0, \pm 1\}$ and a parameter D that defines the number of occurrences of a given z_i in the sum (9). QAOA solves this task by constructing an ansatz

$$|\beta, \gamma\rangle = \prod_{j=1}^p e^{-\beta_j \sum_i X_i} e^{-i\gamma_j C} H^{\otimes n} |0^{\otimes n}\rangle, \quad (10)$$

and optimizing the expectation value $\langle C \rangle = \langle \beta, \gamma | C | \beta, \gamma \rangle$, where C is obtained from C_z by replacing the bits z_u in Eq. (9) by Pauli operators Z_u . In what follows, we evaluate the expectation value

$$\langle C \rangle = \frac{1}{2} \sum_{1 \leq u < v < w \leq n} d_{uvw} \langle \beta, \gamma | Z_u Z_v Z_w | \beta, \gamma \rangle \quad (11)$$

by applying the algorithm introduced earlier to individual terms on the right-hand side of (11).

Following Bravyi et al. [8], we consider an example with $n = 50$ qubits, $p = 1$ (one-layer ansatz), and $\beta = \pi/4$. The expectation value $\langle C \rangle$ is shown as a function of γ in Fig. 1 (top), where each point took only a few seconds to compute on a laptop. In comparison, in [8], generating the same data as in Fig. 1a with the low-rank stabilizer method was reported to take about 3 days. This reflects the fact that whereas sampling from the probability distribution $p(x) = |\langle x | \beta, \gamma \rangle|^2$ is thought to be generically hard, the expectation values (11) can be computed in polynomial time due to the constant depth nature of the circuit, which means that there is a constant size light-cone (with system size). Therefore, this model illustrates the significant simplification afforded if one targets the computation of expectation values with a method that takes advantage of the light-cone structure and the shallow depth. Indeed, even though the whole circuit is composed of $N = \lfloor n \times D/3 \rfloor = 66$

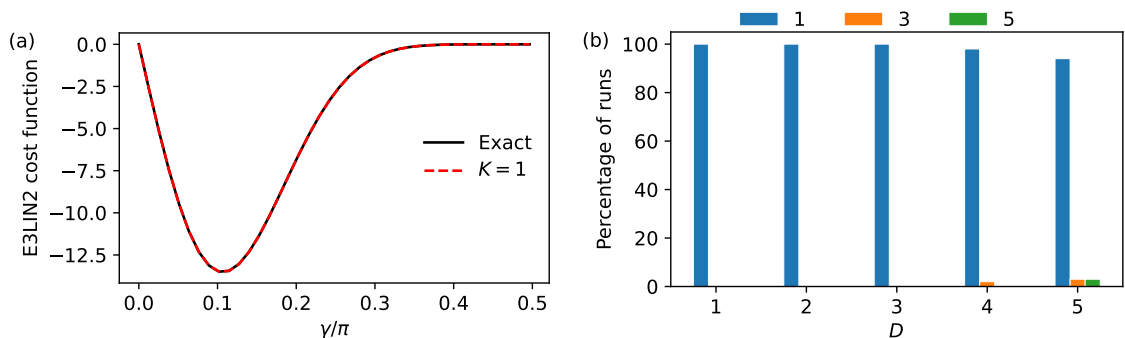


Figure 1: (a) QAOA cost function (11) for the E3LIN2 problem with $n = 50$ qubits and $D = 4$. Only positive values of γ are shown because of the symmetry relation $C(-\gamma) = -C(\gamma)$. (b) Histogram over 100 runs of the maximum order K with a nonzero contribution to the cost function (11) with different values of D and $n = 50$ qubits.

non-Clifford gates, only a fraction of those, namely $\tilde{N} \leq 3(D - 1) + 1$, anticommute with the individual Pauli terms in the observable [21].

However, in Fig. 1a we also show that in this case there is no error if we truncate the perturbation order to $K = 1$, regardless of the value of γ . This arises from the algebraic structure of the gates and observable, which mean that not all operators in the observable lightcone yield a non-zero expectation value, giving additional savings. Prompted by this result, we evaluated randomly generated circuits for $1 \leq D \leq 5$ and for each instance evaluated the number of instances with contributions from higher orders to the expectation value. As seen in Fig. 1b, almost all instances require only the first-order ($K = 1$) perturbation contribution, whereas at higher D there are examples with nonzero third- and fifth-order contributions. These contributions will additionally be weighted by factors of $\tan(\theta)$ which will usually make such terms small. Thus in certain shallow QAOA circuits [22], the perturbation expansion can take advantage of additional truncations and approximations to the observable lightcone, speeding up the classical simulation.

3.2 Coherent error in Clifford circuits

Clifford gates are essential for the implementation of quantum error correction [23] and for the validation of new quantum hardware [1]. Quantum coherent errors introduce a bias in the rotation angles, which implies that simulating such noisy circuits can become difficult because the gates are no longer Clifford. Here, we show that our method can be of use in such cases, especially in the limit of small errors in the rotation angles. Moreover, we show in Appendix B that our approach is applicable to incoherent errors as well, including those represented by Pauli and amplitude- or phase-damping channels.

We construct a Clifford circuit

$$U = \prod_{j=1}^p B_j A_j \quad (12)$$

from alternating layers of one-qubit

$$A = e^{-\frac{i}{2} \sum_{i=1}^n \theta_i \sigma_i} \quad (13)$$

and two-qubit

$$B = e^{-\frac{i}{2} \sum_{i=1}^{n/2} \theta_i P_i}, \quad P_i = \sigma'_{i_1} \sigma''_{i_2} \quad (14)$$

Pauli rotation gates, where $\sigma, \sigma', \sigma'' \in \{X, Y, Z\}$ are selected randomly. In (14), all i_k in the pairs are distinct and chosen randomly, i.e., exactly $n/2$ random disjoint pairs appear within a single two-qubit layer. The rotation angles are set to $\theta \in \{\pm\pi/2, \pm\pi\}$, so that all gates are Clifford. Then, all rotations are distorted ($\theta \rightarrow \theta + \delta\theta$) by $\delta\theta$, which represents the error. We use $n = 50$ qubits and measure the expectation value of $Z_1 Z_{26}$.

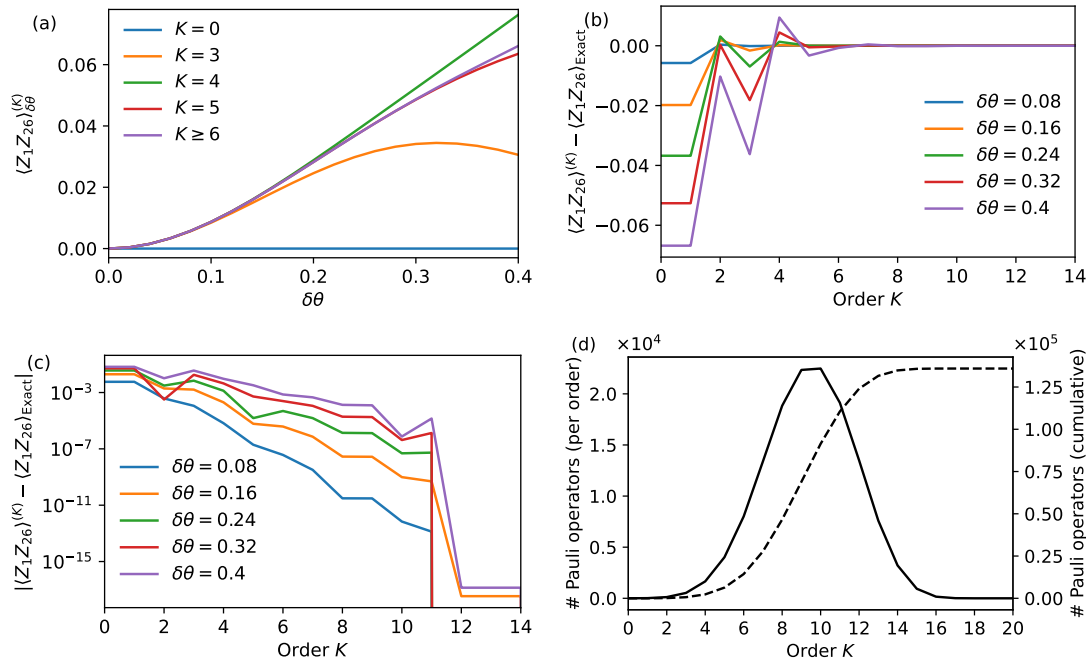


Figure 2: $\langle Z_1 Z_{26} \rangle$ evaluated for a Clifford circuit defined by Eqs. (12)–(14) with $n = 50$ qubits, $p = 4$, and a coherent error defined by $\delta\theta$ (see text). (a) Expectation value as a function of $\delta\theta$ for several perturbation orders K ; (b, c) error in the expectation value as a function of the perturbation order (on linear (b) and logarithmic (c) scales); (d) cumulative (dashed, right-hand axis) and per-order (solid, left-hand axis) number of Pauli operators generated in the evaluation of $\langle Z_1 Z_{26} \rangle$.

Figure 2a plots the expectation value as a function of $\delta\theta$ for different values of perturbation order K . As $\delta\theta$ increases, the expectation value under coherent noise diverges from its noiseless result. Unsurprisingly, the low-order perturbation approach works better for small $\delta\theta$, whereas for larger $\delta\theta$ higher-order perturbation terms are needed. This is shown clearly in Figs. 2b, c. In this example with $p = 4$ (300 gates), we can simulate the expectation values accurately, e.g., with error $< 10^{-2}$, already with $K = 4$ or even $K = 2$ for the smallest values of $\delta\theta$. For comparison, the total number of Pauli operators generated by evolving the observable as $U^\dagger Z_1 Z_{26} U$ is 135930, whereas only 2313 operators are generated for orders up to $K = 4$ (see Fig. 2d).

Next, we illustrate the advantage of carrying out perturbation theory after using the angle transformation on the circuit so that $|\theta| \leq \pi/4$, as outlined in Sec. 2. Figure 3 compares the result from Eq. 2 with and without the angle transformation. Here, the mean absolute error is computed from 1000 examples constructed with $n = 50$ qubits and $p = 3$ layers. Low perturbation orders contribute little to the final expectation values if the rotation gates are not transformed, whereas an opposite trend is observed within the angle transformed picture.

Finally, let us consider an example where performing the exact computation would require extensive computational resources, beyond what can be done with a basic implementation on a personal computer. We set $n = 100$, $p = 3$ (450 gates), and $\delta\theta = 0.2$. The

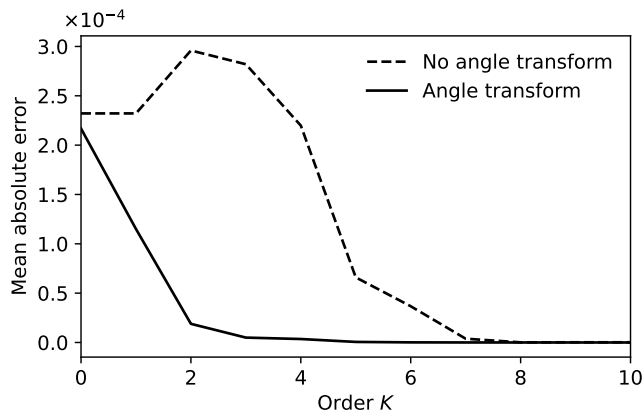


Figure 3: Mean absolute values of errors in $\langle Z_1 Z_{26} \rangle$ for 1000 random circuits generated according to Eqs. (12)–(14) with $n = 50$ qubits, $p = 3$, and $\delta\theta = 0.2$. The results are shown for two different calculations: one in which the perturbation theory is applied directly to the Pauli rotation gates (“no angle transform”) and the other in which the rotation gates are first transformed so that $|\theta| < \pi/4$ (“angle transform”).

calculation up to perturbation order $K = 7$ took approximately 2 hours on a laptop and generated around 10^7 Pauli terms. Given that the expectation values for all $K \geq 4$ are similar, we can estimate $\langle Z_1 Z_{50} \rangle \approx \langle Z_1 Z_{50} \rangle^{(7)} = 0.0023$.

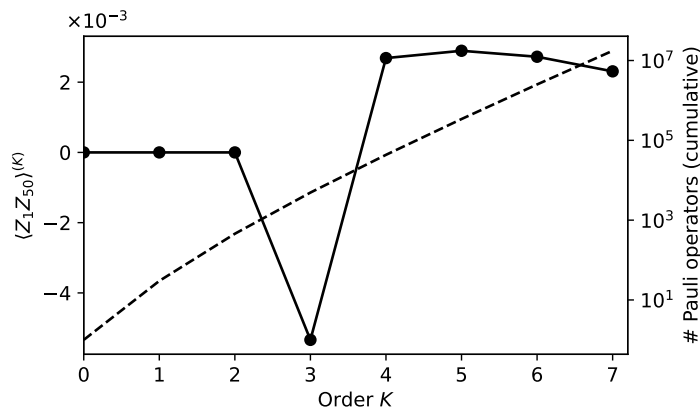


Figure 4: $\langle Z_1 Z_{50} \rangle$ expectation value (solid, left-hand y -axis) for a Clifford circuit ($n = 100$, $p = 3$) with coherent error ($\delta\theta = 0.2$) computed up to perturbation order $K = 7$. The dashed line (right-hand y -axis) shows the total number of Pauli operators generated up to order K .

4 Conclusion

To conclude, we have introduced a Clifford-based perturbation theory that enables the efficient computation of expectation values of near-Clifford quantum circuits. We studied the merits of this approximate scheme in the context of QAOA and Clifford circuits subject to coherent noise. These numerical examples helped illustrate the two sources of speed-up in our method: First, the fact that in some circuits, for example shallow QAOA, only low-order terms in the perturbation expansion are found to be non-zero, and second, the fact that sufficiently small angles of Pauli rotation gates suppress contributions from higher-order terms. In conjunction, these simplifications enable the practical determination of

expectation values of observables of large near-Clifford circuits, for example, with over a hundred qubits and hundreds of gates, using only laptop computational resources.

5 Acknowledgments

We acknowledge informative discussions with Steve Flammia, Ali Lavasani, David Gosset, Sergey Bravyi, and Alex Dalzell. TB and GKC were supported by the US Department of Energy, Office of Science, Office of Advanced Scientific Computing Research and Office of Basic Energy Sciences, Scientific Discovery through Advanced Computing (SciDAC) program under Award Number DE-SC0022088. TB acknowledges financial support from the Swiss National Science Foundation through the Postdoc Mobility Fellowship (grant number P500PN-214214). GKC is a Simons Investigator in Physics.

A Random quantum circuits

Let us consider a random quantum circuit composed of Pauli rotations with a fixed small angle $\theta_i = \theta$, such that $\cos(\theta) \approx 1$. Then,

$$E^{(k)} = i^k \sin^k(\theta) \sum_{1 \leq j_1 < \dots < j_k \leq \tilde{N}} \langle 0^{\otimes n} | P_{j_k} \dots P_{j_1} O | 0^{\otimes n} \rangle. \quad (15)$$

In the remainder, we will not discuss the value of $i^k \langle 0^{\otimes n} | P_{j_k} \dots P_{j_1} O | 0^{\otimes n} \rangle \in \{0, \pm 1\}$, but rather focus on the average value of the sum of absolute values of the coefficients

$$|E|^{(k)} = M^{(k)} |\sin(\theta)|^k, \quad (16)$$

where $M^{(k)}$ denotes the average number of Pauli operators at perturbation order k . We can deduce $M^{(k)}$ by assuming that the Pauli rotation gate $U_{i+1}(\theta)$ commutes with each term in the evolved observable O_i with a probability of 0.5. Let us label one Pauli operator in O_i as $o_i^{(k)}$, where k indicates the number of times it has been multiplied by $\sin(\theta)$, i.e., its order. If $[P_{i+1}, o_i^{(k)}] = 0$, according to Eq. (3), $U_{i+1}(\theta)^\dagger o_i^{(k)} U_{i+1}(\theta) = o_i^{(k)}$, i.e., the number of terms remains the same. Otherwise, if $\{P_{i+1}, o_i^{(k)}\} = 0$, $U_{i+1}(\theta)^\dagger o_i^{(k)} U_{i+1}(\theta) = \cos(\theta) o_i^{(k)} + i \sin(\theta) P_{i+1} o_i^{(k)}$. Here, the number of Pauli operators of order k remains the same, but the number of terms of order $k+1$ is increased by 1. This results in the following recursive formula

$$M_i^{(k)} = M_{i-1}^{(k)} + \frac{1}{2} M_{i-1}^{(k-1)}, \quad (17)$$

where $M_i^{(k)}$ denotes the number of terms of order k in the observable O_i evolved up to step i and $M_0^{(k)} = \delta_{k0}$. By induction, we can prove the following closed-form expression

$$M^{(k)} = M_N^{(k)} = 2^{-k} \binom{N}{k}, \quad (18)$$

which agrees with the average total number of Pauli operators $M = \sum_{k=0}^N M^{(k)} = (3/2)^N$. Then,

$$|E|^{(k)} = |\sin(\theta)/2|^k \binom{N}{k} \quad (19)$$

and

$$|O|^{(K)} = \sum_{k=0}^K |E|^{(k)} = \sum_{k=0}^K |\sin(\theta)/2|^k \binom{N}{k}. \quad (20)$$

In particular,

$$|O| = |O|^{(N)} = (1 + |\sin(\theta)/2|)^N. \quad (21)$$

Let us now consider an upper bound on the relative error

$$\frac{|O| - |O|^{(K)}}{|O|} < \delta. \quad (22)$$

Specifically, we wish to find the smallest value of perturbation order K that satisfies the equation above for given N , θ , and δ . As an example, Fig. 5 shows K as a function of N for $\delta = 0.01, 0.05$, and $\theta = 0.2$.

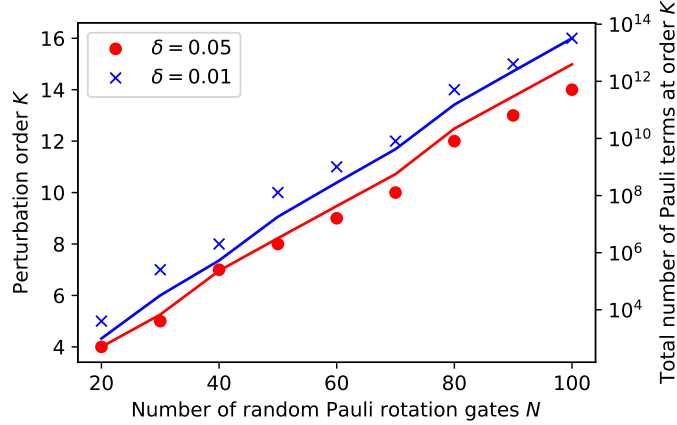


Figure 5: Minimal value of the perturbation order K that satisfies Eq. (22) for different numbers of gates N , angle $\theta = 0.2$, and $\delta = 0.05$ (red markers) or $\delta = 0.01$ (blue markers). Solid lines (right-hand y -axis) correspond to $\sum_{k=0}^K M^{(k)}$ for each pair of N and K .

B A note on incoherent errors

Several basic models of errors [24] can be represented as a Pauli channel

$$\tilde{\rho} = (1 - s_x - s_y - s_z)\rho + s_x X\rho X + s_y Y\rho Y + s_z Z\rho Z, \quad (23)$$

including bit flip errors

$$\tilde{\rho} = (1 - s)\rho + sX\rho X, \quad (24)$$

phase flip errors

$$\tilde{\rho} = (1 - s)\rho + sZ\rho Z, \quad (25)$$

and a depolarizing channel

$$\tilde{\rho} = (1 - s)\rho + \frac{s}{3}(X\rho X + Y\rho Y + Z\rho Z). \quad (26)$$

Pauli channels can be implemented with our method deterministically and at almost no additional computational cost. First, we note that the Pauli operators and the scaling factor in Eq. (23) can be applied directly to the observable (i.e. in the Heisenberg picture) instead of on the density operator. Second, the conjugation of one Pauli operator by another results only in a potential sign change:

$$\sigma_{\text{Error}}\sigma_{\text{Observable}}\sigma_{\text{Error}} = \pm\sigma_{\text{Observable}}, \quad (27)$$

where the sign depends on whether the two Pauli operators commute. Therefore, a one-qubit Pauli channel applied to a Pauli operator will only introduce a scaling factor

$$\eta = 1 - s_x - s_y - s_z \pm s_x \pm s_y \pm s_z. \quad (28)$$

Another example is the amplitude-damping error [24], which can be represented as:

$$\tilde{\rho} = E_0^\dagger \rho E_0 + E_1^\dagger \rho E_1, \quad (29)$$

where

$$E_0 = \begin{pmatrix} 1 & 0 \\ 0 & \sqrt{1-\lambda} \end{pmatrix}, \quad (30)$$

$$E_1 = \begin{pmatrix} 0 & \sqrt{\lambda} \\ 0 & 0 \end{pmatrix}. \quad (31)$$

Equation (29) applied to single-qubit Pauli operators yields:

$$\tilde{I} = I \quad (32)$$

$$\tilde{X} = \sqrt{1-\lambda}X \quad (33)$$

$$\tilde{Y} = \sqrt{1-\lambda}Y \quad (34)$$

$$\tilde{Z} = (1-\lambda)Z + \lambda I. \quad (35)$$

I , X , and Y can be efficiently simulated, but any occurrence of Z will produce twice as many Pauli terms. Fortunately, the two branches in the last equation have different weights if λ is small, so the problem can be again treated perturbatively by keeping track of powers of λ .

Finally, the phase-damping channel can be simulated efficiently. It is similar to the amplitude damping channel [Eq. (29)] but with

$$E_0 = \begin{pmatrix} 1 & 0 \\ 0 & \sqrt{1-\lambda} \end{pmatrix}, \quad (36)$$

$$E_1 = \begin{pmatrix} 0 & 0 \\ 0 & \sqrt{\lambda} \end{pmatrix}. \quad (37)$$

The application to Z now leaves it unchanged ($\tilde{Z} = Z$), while the action on all other operators is the same as in the amplitude-damping channel [Eqs. (32)–(34)]. Therefore, the phase-damping channel can be simulated at no additional cost.

References

- [1] Andrew W. Cross, Lev S. Bishop, Sarah Sheldon, Paul D. Nation, and Jay M. Gambetta. “Validating quantum computers using randomized model circuits”. *Phys. Rev. A* **100**, 032328 (2019).
- [2] Daniel Gottesman. “The Heisenberg Representation of Quantum Computers” (1998). arXiv:9807006.
- [3] Scott Aaronson and Daniel Gottesman. “Improved simulation of stabilizer circuits”. *Phys. Rev. A* **70**, 052328 (2004).

- [4] Maarten Van Den Nest. “Classical Simulation of Quantum Computation, the Gottesman-Knill Theorem, and Slightly Beyond”. *Quantum Info. Comput.* **10**, 258–271 (2010).
- [5] Sergey Bravyi and David Gosset. “Improved Classical Simulation of Quantum Circuits Dominated by Clifford Gates”. *Phys. Rev. Lett.* **116**, 250501 (2016).
- [6] Ryan S. Bennink, Erik M. Ferragut, Travis S. Humble, Jason A. Laska, James J. Nutaro, Mark G. Pleszkoch, and Raphael C. Pooser. “Unbiased simulation of near-Clifford quantum circuits”. *Phys. Rev. A* **95**, 062337 (2017).
- [7] Hammam Qassim, Joel J. Wallman, and Joseph Emerson. “Clifford recompilation for faster classical simulation of quantum circuits”. *Quantum* **3**, 170 (2019).
- [8] Sergey Bravyi, Dan Browne, Padraic Calpin, Earl Campbell, David Gosset, and Mark Howard. “Simulation of quantum circuits by low-rank stabilizer decompositions”. *Quantum* **3**, 181 (2019).
- [9] Yifei Huang and Peter Love. “Feynman-path-type simulation using stabilizer projector decomposition of unitaries”. *Phys. Rev. A* **103**, 022428 (2021).
- [10] Aleks Kissinger and John van de Wetering. “Simulating quantum circuits with zx-calculus reduced stabiliser decompositions”. *Quantum Sci. Technol.* **7**, 044001 (2022).
- [11] Sergey Bravyi, David Gosset, and Ramis Movassagh. “Classical algorithms for quantum mean values”. *Nat. Phys.* **17**, 337–341 (2021).
- [12] M. Cerezo, Andrew Arrasmith, Ryan Babbush, Simon C. Benjamin, Suguru Endo, Keisuke Fujii, Jarrod R. McClean, Kosuke Mitarai, Xiao Yuan, Lukasz Cincio, and Patrick J. Coles. “Variational quantum algorithms”. *Nat. Rev. Phys.* **3**, 625–644 (2021).
- [13] Alberto Peruzzo, Jarrod McClean, Peter Shadbolt, Man-Hong Yung, Xiao-Qi Zhou, Peter J. Love, Alán Aspuru-Guzik, and Jeremy L. O’Brien. “A variational eigenvalue solver on a photonic quantum processor”. *Nat. Commun.* **5**, 4213 (2014).
- [14] Edward Farhi, Jeffrey Goldstone, and Sam Gutmann. “A quantum approximate optimization algorithm” (2014). arXiv:1411.4028.
- [15] Edward Farhi and Aram W Harrow. “Quantum Supremacy through the Quantum Approximate Optimization Algorithm” (2016). arXiv:1602.07674.
- [16] Nikita A. Nemkov, Evgeniy O. Kiktenko, and Aleksey K. Fedorov. “Fourier expansion in variational quantum algorithms” (2023). arXiv:2304.03787.
- [17] Kosuke Mitarai, Yasunari Suzuki, Wataru Mizukami, Yuya O. Nakagawa, and Keisuke Fujii. “Quadratic Clifford expansion for efficient benchmarking and initialization of variational quantum algorithms”. *Phys. Rev. Res.* **4**, 033012 (2022).
- [18] Qiskit contributors. “Qiskit: An open-source framework for quantum computing” (2023).
- [19] Edward Farhi, Jeffrey Goldstone, and Sam Gutmann. “A Quantum Approximate Optimization Algorithm Applied to a Bounded Occurrence Constraint Problem” (2015). arXiv:1412.6062.
- [20] Yingkai Ouyang. “Avoiding coherent errors with rotated concatenated stabilizer codes”. *npj Quantum Inf.* **7**, 87 (2021).

- [21] Patrick Rall, Daniel Liang, Jeremy Cook, and William Kretschmer. “Simulation of qubit quantum circuits via Pauli propagation”. *Phys. Rev. A* **99**, 062337 (2019). arXiv:1901.09070.
- [22] Wei-Feng Zhuang, Ya-Nan Pu, Hong-Ze Xu, Xudan Chai, Yanwu Gu, Yunheng Ma, Shahid Qamar, Chen Qian, Peng Qian, Xiao Xiao, Meng-Jun Hu, and Dong E. Liu. “Efficient Classical Computation of Quantum Mean Values for Shallow QAOA Circuits” (2021). arXiv:2112.11151.
- [23] Sergey Bravyi, Joseph A. Latone, and Dmitri Maslov. “6-qubit optimal Clifford circuits”. *npj Quantum Inf.* **8**, 79 (2022).
- [24] Michael A. Nielsen and Isaac L. Chuang. “Quantum computation and quantum information”. Cambridge University Press. Cambridge (2010).